ECCOMAS Congress 2016
VII European Congress on Computational Methods in Applied Sciences and Engineering
M. Papadrakakis, V. Papadopoulos, G. Stefanou, V. Plevris (eds.)
Crete Island, Greece, 5–10 June 2016

# SEISMIC RETROFIT OF AN INDUSTRIAL STRUCTURE THROUGH AN INNOVATIVE SELF-CENTERING HYSTERETIC DAMPER: MODELLING, ANALYSIS AND OPTIMIZATION

**F. Morelli**[1], **A. Piscini**[1], **W. Salvatore**[1]

[1] University of Pisa, Department of Civil and Industrial Engineering
Largo Lucio Lazzarino 1, 56122, Pisa, Italy
{francesco.morelli, andrea.piscini, walter}@ing.unipi.it

**Keywords:** seismic risk, industrial building, self-centering, seismic energy, energy dissipation.

**Abstract.** *Recent earthquakes, as the one that hit Fukushima in Japan in 2011 or the one that produced extensive damage in Turkish petrochemical facilities during the Kocaeli earthquake of 1999 or, more recently, the seismic events in May 2012 in Emilia (Italy), highlighted the increasing need of providing adequate protection to industrial installations. Industrial facilities often store a large amount of hazardous material and, in case of seismic event, there is a high probability that accidental scenarios as fire, explosion, toxic or radioactive dispersion may occur. In these cases, the ensuing disaster certainly harms the people working in the installation and it may endanger the population living in the neighborhood or in the urban area where the industrial installation is located. The consequences of such accidental scenarios can be disastrous in terms of casualties, economic losses and environmental damage. Within this work, the seismic behavior of an industrial structure is studied through several Incremental Dynamic Analyses, IDA, and particular attention is given to the selection of suitable performance criteria and the modelling of non linear phenomena (II order effects, buckling, mechanical non-linearity, etc.). The seismic behavior is then enhanced applying to the structure an innovative typology of self-centering hysteretic damper, whose mechanical characteristics are optimized through the execution of IDAs on the retrofitted structures. A final comparison between the seismic behavior of the original structure and of the retrofitted one highlights the advantages of the innovative self-centering hysteretic dampers.*

## 1 INTRODUCTION

Recent earthquakes, as the one that hit Fukushima in Japan in 2011, the one that produced extensive damage in Turkish petrochemical facilities during the Kocaeli earthquake of 1999 or, more recently, the seismic events in May 2012 in Emilia (Italy), highlighted the increasing need of providing adequate protection to industrial installations.

Industrial facilities often store a large amount of hazardous material and, in case of seismic event, there is a high probability that accidental scenarios as fire, explosion, toxic or radioactive dispersion may occur. In these cases, the ensuing disaster certainly harms the people working in the installation and it may endanger the population living in the neighbourhood or in the urban area where the industrial installation is located. The consequences of such accidental scenarios can be disastrous in terms of casualties, economic losses and environmental damage.

Even in the cases in which the content does not represent a direct threat to human lives or to the environment, damage to structural and/or non structural elements can result in huge indirect economic losses, as testified from the numerous studies [1] [2] devoted to the speedup of community recovery after the 2012 Emilia (Italy) earthquakes. From his point of view, for industrial buildings, it should be more appropriate to speak about "seismic resilience" than "seismic risk", that is more appropriate for civil building [3], meaning that it is necessary to take into account also the time necessary for the recovery of the production activities.

In this field, a parameter strictly correlated to the post-earthquake recovery is represented by the re-centering capability of the structure, defined as the capacity of minimizing the residual displacement after the end of the seismic action.

In this contest, a particular attention for the retrofit of existing industrial plants is given to the use of passive dissipation systems, such as Isolation Systems (IS) or Energy Dissipation Systems (EDS). The initial higher cost associate to a retrofit using an IS or EDS, comprised the ones consequent to the adaptation of the non-structural elements (e.g. pipelines), will be likely compensate by the avoided losses in case of moderate-to-strong earthquakes. This is especially true for industrial steel structures, where the substitution of the existing bracing elements with dissipative ones can be accomplished using simple operations. Modern codes [4] and guidelines [5] lists the recentering capability of the anti-seismic device as one of the fundamental capacities. In [5] it is evaluated, for linear analysis and seismically isolated structures, comparing the energy dissipated by the isolation device, $E_H$, with the reversibly stored (elastic strain and potential) energy, $E_S$ :

$$E_S \geq 0.25 E_H \qquad (1)$$

Traditional hysteretic devices, however, does not provide a real "active" recentering force, resulting in the presence of residual forces within the devices at the end of the earthquake also in the case of negligible residual displacement and in the consequent complication of the substitution operations.

In order to mitigate such problems, re-centering devices have been the object of ever increasing research study ([6], [7], [8], [9], [10], [11], [12]). This type of dissipative device is characterized by the presence of a re-centering force that mitigates, and may even eliminate, the residual deformations in buildings and residual forces in the dissipative devices after earthquakes.

In the present paper, the influence, in terms of maximum displacement, interstorey drift, acceleration and dissipated energy, of the retrofit of an existing industrial steel building using the steel self-centering device (SSCD) developed in [13] is studied. The industrial building, selected within one of the most important Italian industrial plant, the ILVA S.p.A. plant, can

be considered as representative of the industrial structure sensitive to the seismic action, being characterized by an important mass placed at high altitude.

The case study building analysis is carried out indentifying, in the first phase, the structural and non-structural limit states, considering both the national and international standards and the peculiarity of the building itself. Given the need of simplifying, as much as possible, the structural scheme to obtain a reliable and time-saving nonlinear model, a preliminary comparison between a full-comprehensive linear model and the geometrically-simplified one is carried out, studying also the effect of the infill material modelling on the overall behavior. Several IDA are then carried out in order to identify the main seismic vulnerabilities, to define the seismic retrofit intervention and evaluate their effects on the structural behavior.

## 2 CASE STUDY DESCRIPTION: MODELLING, ANALYSIS AND SEISMIC VULNERABILITY

The selected case study, shown in Figure 1, has the function of filtering the gasses coming from the steelwork and can be schematized as made up of a supporting structure, the silos containing the filtering material and the roof.

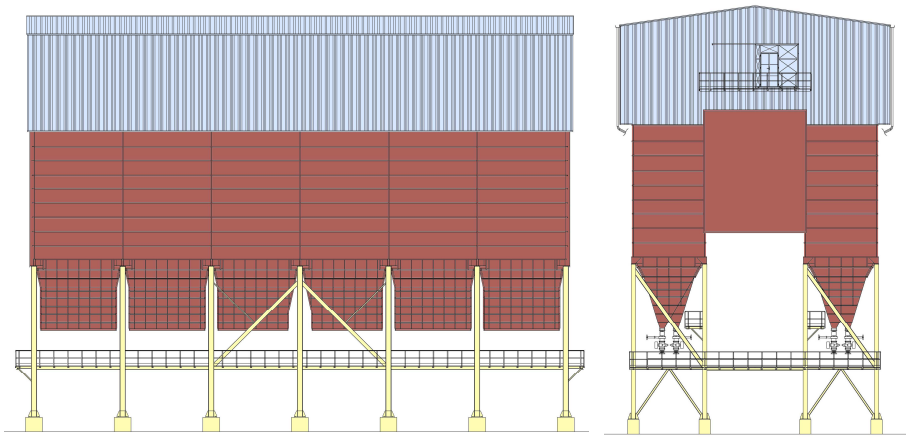

Figure 1. Front and lateral view of the Filter Building

The building has a regular plan, with overall dimensions 37.80 m x 16.94 m and total height 29.64m. The supporting structure, with a total height of about 10.80 m, has six bays in the longitudinal direction and three in the transversal one. Different horizontal resisting systems can be individuated such as moment resisting frames, inverted V bracings, diagonal bracings, as shown in Figure 2 .

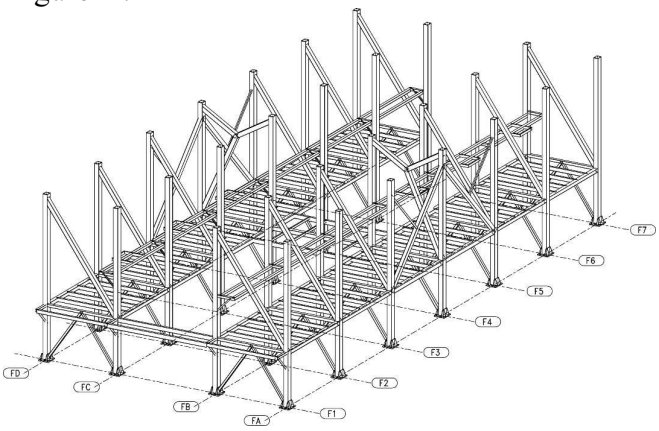


Figure 2. 3D view of the supporting system

The silos are realized with thin (4 mm) walls stiffened with a close series of horizontal UPN and vertical HEA profiles. The total mass of the silo (23700 kN), considering structural elements and infill material, represent the 86% of the total mass (27650 kN).

The roof is connected directly to the filter walls and its contribution is considered only in terms of vertical load and mass.

### 2.1 Linear and non linear modelling

To develop a suitable nonlinear model of the building for the execution of Incremental Dynamic Analyses, IDAs, in reasonable amount of time, it is necessary to simplify the structural scheme. In order to have, however, a model able to well represent the structural behavior, it is initially studied a "complete" linear model, see Figure 3a), in which the contribution of practically almost all the structural and non-structural elements is taken into account.

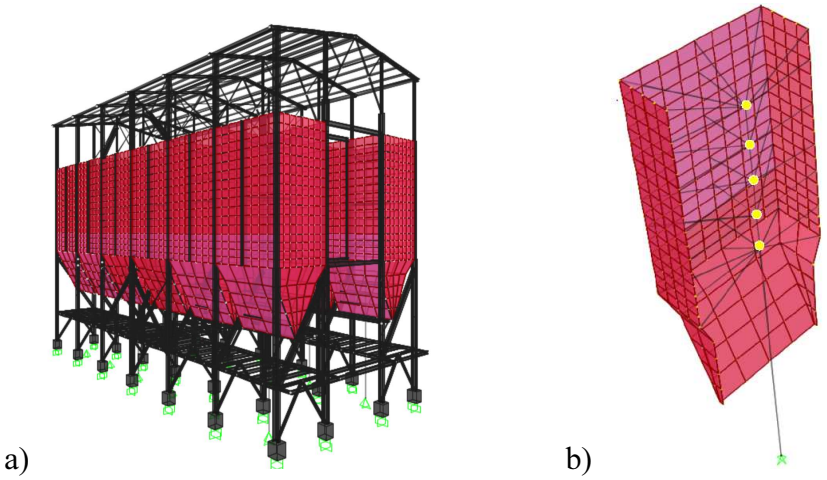

a) b)

Figure 3. "Complete" linear model: a) globall view; b) modelling of the infill-silo interaction.

The dynamic interaction between the silos wall-infill material can sensibly vary the global response of the building. Given the high level of uncertainty associated to the infill material behavior, similar to dust, a refined non-linear interaction model would lead to non-reliable results. For this reason, different infill material modelling solutions are studied and compared and a parametric study is carried out to study the sensitivity of the global behavior to the variation of the characteristics of the schematization assumed.

Three different types of modelling are compared: i) the attribution of the infill material mass directly to the silos walls; ii) the concentration of the infill material total mass of each silo in a single point placed in the baricenter of the silo and connected to the silos walls by linear springs; iii) subdivision of the infill material total mass in 5 points, see Figure 3b), each one of them connected to the silos walls by linear springs. Models i) and ii) highlighted several drawbacks, such as, for the former, the unrealistic high number of the silos walls local vibration modes and the problem of overestimating the rotational inertia, while, for the latter, the high force concentration on the silos wall. The model iii) is then assumed and a parametric analysis varying the spring stiffness is carried out and the results, in terms of period of vibration and participating mass is reported in Figure 4.

It can been noticed that for infill material edometric modulus higher than 25000 kN/m$^2$, the period and the participating mass associated to the first period can be considered practically constant. Given that the edometric modulus of the dust varies, approximately, between 30000 to 80000 kN/m$^2$, the response of the model can be assumed to be not influenced by the uncertainties related to the infill material mechanical behavior.

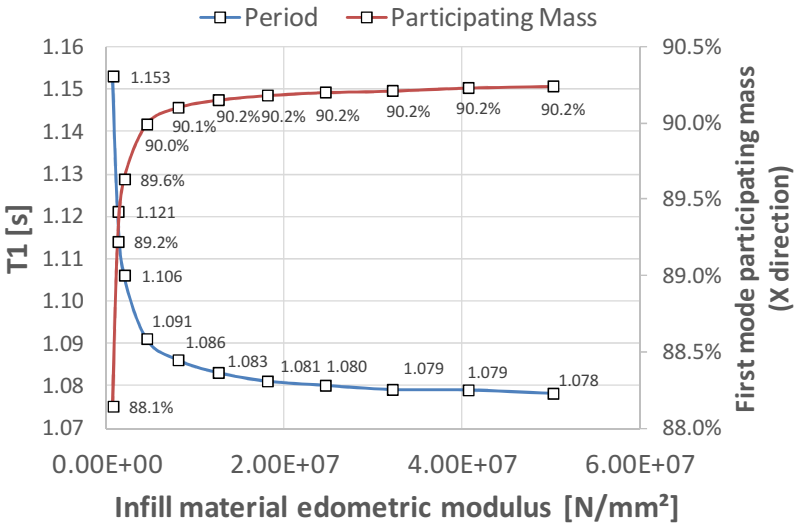


Figure 4. Period of vibration and participanting mass associate to the first vibration period varying the stiffness of the connecting spring in model iii)

The linear model described highlights a structural behavior similar to the one of a single degree of freedom (SDOF), where the great part of the displacement demand is located in the supporting structure. The silos and the roof behave such as a rigid body and the resultant stresses are far below the yielding or buckling threshold. For this reason the structural behavior can be represented by the simplified model shown in Figure 5, where the roof is considered simply as dead load and mass, while the silos are substituted by a trusses system, whose characteristics are evaluated to obtain the same first period and modal shape of the "complete" model.

The simplified model is used to perform the nonlinear IDAs. Each element is modelled using a fiber element and the material is assumed to be elasto-plastic. The global second-order effects are explicitly taken into account, while, in order to consider the post-critic behavior of the bracings in compression, they are modelled introducing the initial imperfection as foreseen by Eurocode 3 [14]. The viscous damping is taken into account introducing an damping ratio associated to the first and second vibrating modes equal to 2% and setting the damping matrix proportional to the mass and initial stiffness matrix.

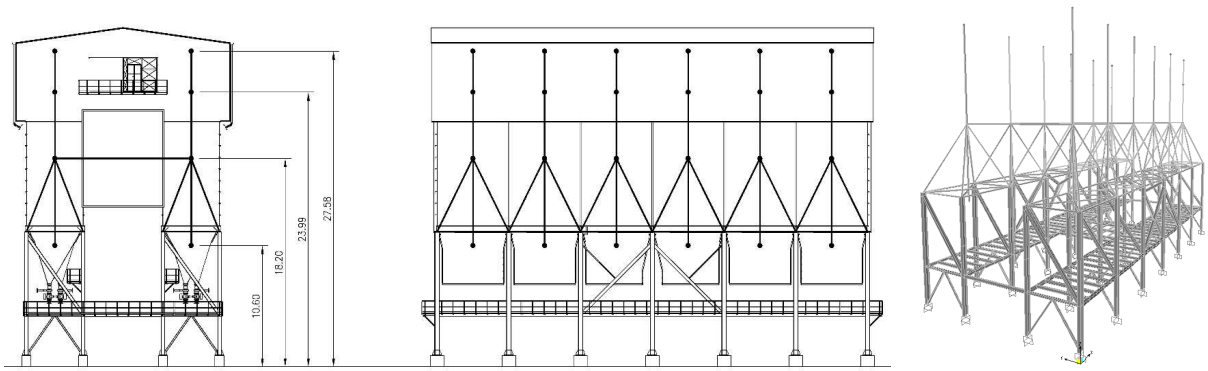


Figure 5. Case study building simplified model

## 2.2 Limit states and performance parameters

The Ultimate Limit State considered during the structural analysis are resumed, together with the reference standard, in following table .

| ULTIMATE LIMIT STATE | ELEMENT | CHECK | STANDARD |
|---|---|---|---|
| Shear resistance | Column | $V_{Ed} / V_{pl,Rd} \leq 0.50$ | EN 1998-1:2013 [15] |
| Plastic rotation capacity | Columns | $\phi < \phi_u$ | EN 1998-3:2005 |
| Plastic rotation capacity | Beams | $\phi < \phi_u$ | EN 1998-3:2005 |
| Axial deformation capacity in tension and compression | Dissipators/ Bracings | $\Delta L < \Delta Lc$ (compression/buckling)<br>$\Delta L < \Delta Ly$ (tension) | EN 1998-3:2005 |
| Check of sensibility coefficient Theta | Global | $\vartheta < 0.3$ | EN 1998-1:2013 [15] |
| Maximum displacement | Global | dr < 0.50m<br>Due to the interaction with non structural elements | -- |

Table 1. Main limit state considered

To evaluate the building performance, four different parameters are evaluated during the IDA analysis:

1. maximum displacement. Related to the non structural elements (such as external cladding) damage;
2. maximum acceleration. Related to the acceleration-sensitive systems damage;
3. residual deformation. Related to the structural damage and resilience;
4. seismic energy. The different components of the energy supply important information on the structural damage and on the retrofit choices.

In particular, four type of seismic energy are analyzed: input energy, defined as the energy transmitted by the ground movement to the structure; kinetic energy, related to the building movements; adsorbed (strain + dissipated) energy, related to the damaging of the structure; viscous energy.

## 2.3 Selection of ground motions

In order to achieve the worst damage scenarios with a robust and reliable procedure, an Uniform Hazard Spectrum -coherent method is adopted for the ground motions. The complete procedure, together with all the background and motivations, is described in the paper presented by Faggella et al. at the 2016 ECCOMAS conference "Performance-based Nonlinear Response History Analysis Framework for the “PROINDUSTRY” Project Case Studies".

A major drawback of using unscaled GMs is that a higher number of records need to be used. At least 7 GMs are needed but, considered their high variation, a higher number is preferred, at least equal to 11. The selected ground motions are listed in Table 2. The IDAs are executed applying simultaneously the three components (2 horizontal and 1 vertical) of each ground motion and using 9 scale factors, SFs, see Figure 6. A total of 198 nonlinear time-history analyses are carried out for the case study (11 GMs x 9 SFs x 2 directional combinations).

| DB | ID | Earthquake Name | Mw | Fault Mec. | R(kM) | Site Class | Date |
|---|---|---|---|---|---|---|---|
| **ED** | 6349 | South Iceland | 6,4 | Strike slip | 5 | A | 21/06/2000 |
| **ED** | 196 | Montenegro | 6,9 | Thrust | 25 | B | 14/04/1979 |
| **ED** | 535 | Erzincan | 6,6 | Strike slip | 13 | B | 13/03/1992 |
| **ED** | 74 | Gazli | 6,7 | Thrust | 11 | D | 17/05/1976 |
| **ED** | 1257 | Izmit | 7,6 | Strike slip | 20 | C | 17/08/1999 |
| **IN** | 113 | South Iceland | 6,5 | Strike slip | 5,25 | A | 17/06/2000 |
| **IN** | 466 | Duzce | 7,1 | Strike slip | 5,27 | C | 12/11/1999 |
| **IN** | 331 | Darfield | 7,1 | Strike slip | 17,82 | C | 03/09/2010 |
| **IN** | 445 | Imperial Valley | 6,5 | Strike slip | 27,03 | C | 15/10/1979 |
| **IN** | 451 | Loma Prieta | 6,9 | Oblique | 7,1 | B | 18/10/1989 |
| **IN** | 461 | Northridge | 6,7 | Reverse | 20,25 | C | 17/01/1994 |

Table 2. Ground motions selected for the execution of IDAs

| REGGIO CALABRIA | | | | | | |
|---|---|---|---|---|---|---|
| | Vr | $P_{vr}$ | λ | Tr | ag | S.F. |
| | yrs | % | 1/yrs | yrs | g | \ |
| 0 | 100 | 4% | 0.0004 | **2475** | 0.512 | 1.43 |
| 1 | 100 | **5%** | 0.0005 | 1950 | 0.4687 | 1.307 |
| 2 | 100 | **10%** | 0.0011 | 949 | 0.3586 | **1.000** |
| 3 | 100 | 22% | 0.0025 | 402 | 0.2502 | 0.698 |
| 4 | 100 | 30% | 0.0036 | 280 | 0.2122 | 0.592 |
| 5 | 100 | 39% | 0.0049 | 202 | 0.1829 | 0.510 |
| 6 | 100 | 50% | 0.0069 | 144 | 0.1552 | 0.433 |
| 7 | 100 | **63%** | 0.0099 | 101 | 0.1292 | 0.360 |
| 8 | 100 | **81%** | 0.0166 | 60 | 0.0987 | 0.275 |

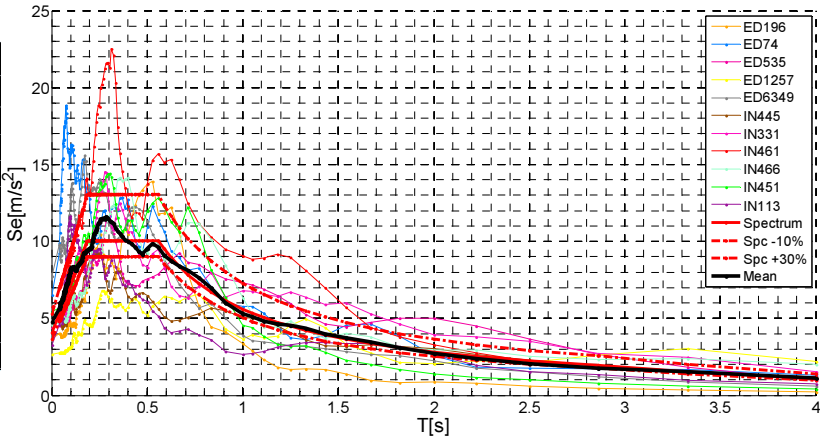


Figure 6. Selected ground motions response spectrum and Scale Factor, S.F., used

## 2.4 Seismic vulnerability of the case study current state

The seismic vulnerability of the case study is studied through the IDAs and represented through the IDA curves, in terms of maximum displacement, maximum acceleration, residual displacement and seismic energy (elastically stored or dissipated by the structure). All the parameters are registered at three different levels of the structure, see Figure 7.

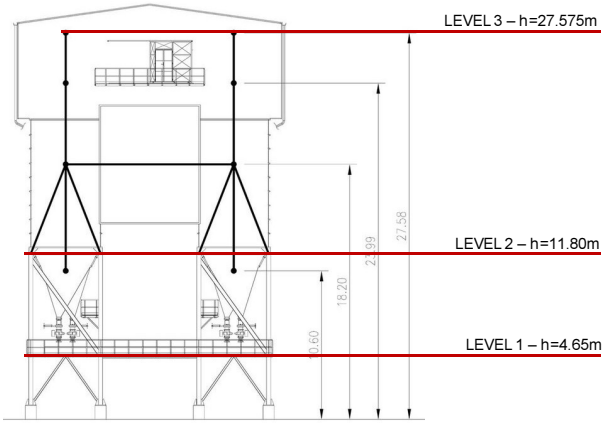


Figure 7. Individuation of recorded levels

In Figure 8 and Figure 9, the IDA curves more representative of the strucruarl behavior are shown, while in Figure 10 the maximum displacements versus the maximum shear force plotted.

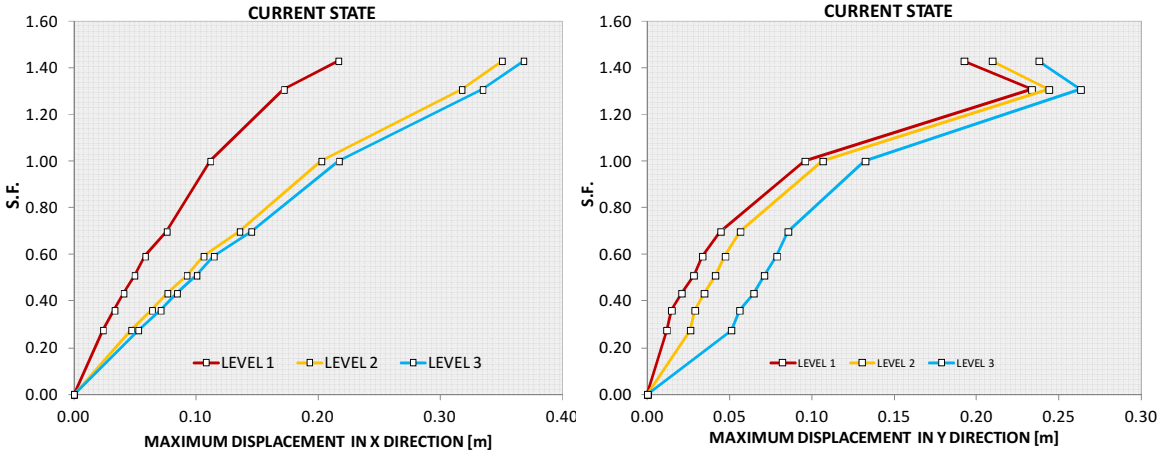


a) b)

Figure 8. Maximum displacements (mean values) at different level in the a) X and b) Y directions

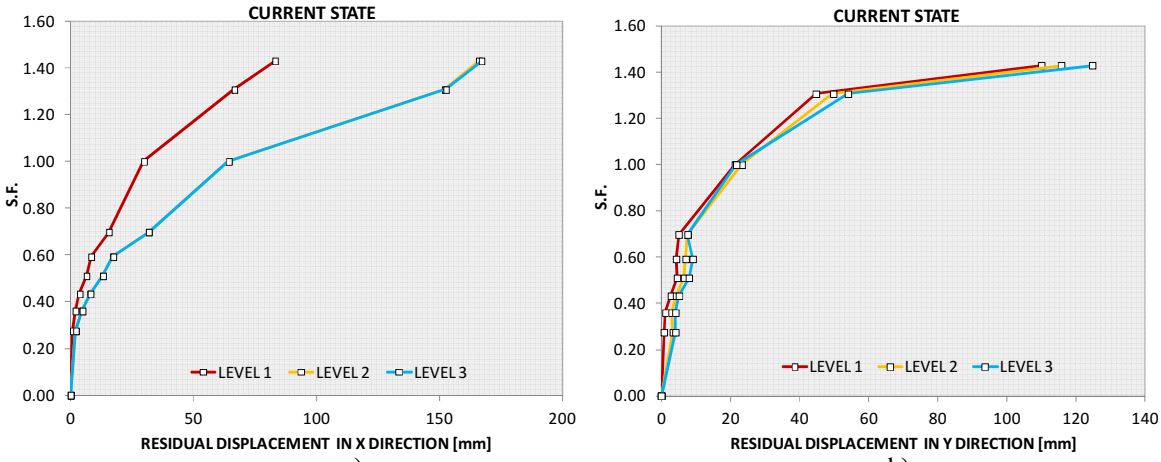


a) b)

Figure 9. Residual displacements (mean values) at different level in the a) X and b) Y directions

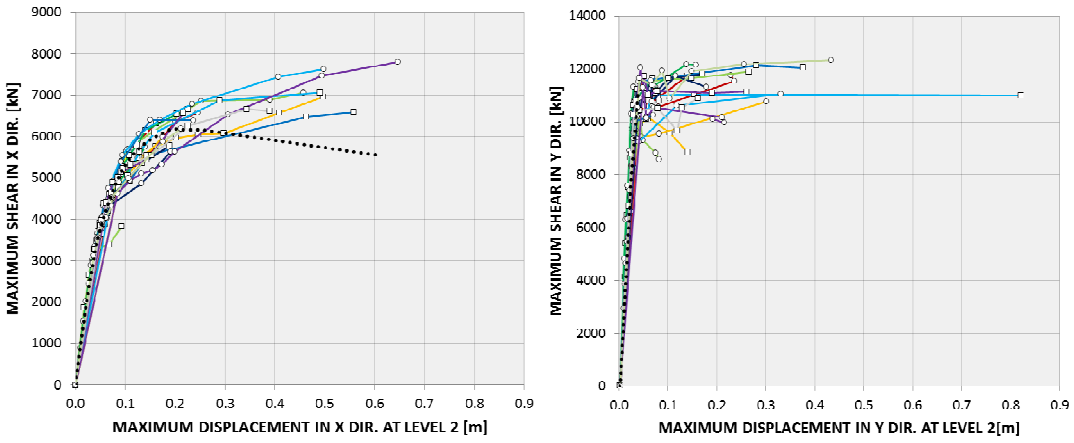


a) b)

Figure 10. Maximum base shear vs maximum displacement at level 2 graph in the a) X direction and b) Y direction

From the analysis of Figure 8 and Figure 9 it can be seen that, in the X direction the displacement demand is equally distributed between the ground and first floor. This is mainly due to the low number of bracing in the first floor. In the Y direction, the displacement demand is concentrated at the ground floor, highlighting an early plasticization of the inverted V bracings with respect to the first floor diagonal bracings. In both directions, important residual displacements are registered at the end of each time-history analysis. The presence of such residual displacements lower considerably the resilience of the building, given the great difficulties in repairing a deformed and unstable structure.

Interesting information on the building behavior, especially in view of the retrofitting study and optimization, are supplied by the analysis of the input seismic energy transmitted by the earthquake to the structure and the stored and/or dissipated one. In Figure 11 an example of the energy time-histories recorded for the ground motion IN113A (the final A means that the main horizontal component is applied in the X direction) are reported for two different scale factors. It can be observed that, for low SCs, the energy dissipation takes place mainly for viscous damping, while, increasing the seismic action, the energy adsorbed by the structure, strictly related to the structural damage, represent the main component of the input energy.

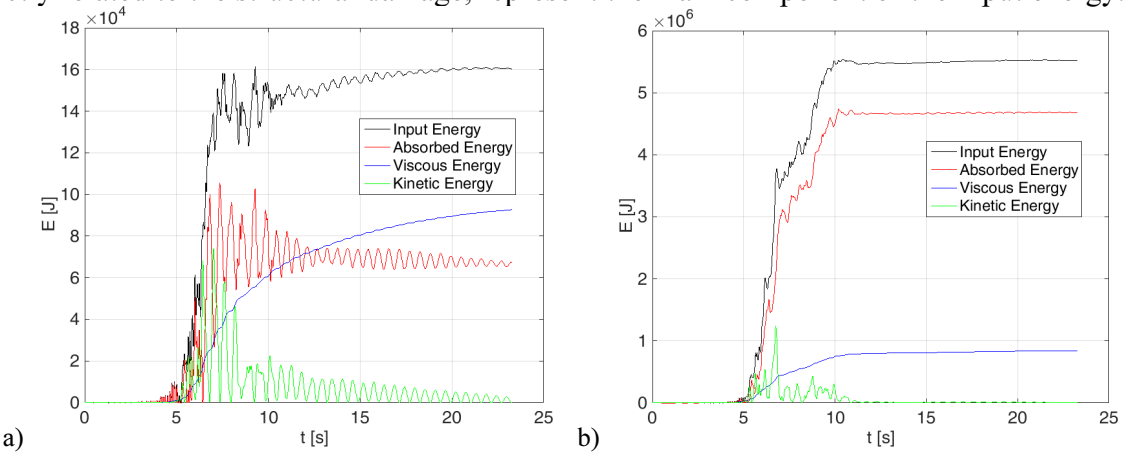


Figure 11. Energy time-histories for the IN113A GM recording: a) SF = 0.275; b) SF= 1.430.

Interesting results can be obtained comparing the ratio between the adsorbed or the viscous energy and the input one for all the GMs and SFs considered, as shown in Figure 12. It can be noticed, in fact, that for all the GMs the ratio with the input energy tends to a certain value, respectively equal to 0.83 for the adsorbed and 0.17 for the viscous energy. This means that, for SFs higher than 0.592 the structure develops the complete collapse mechanism.

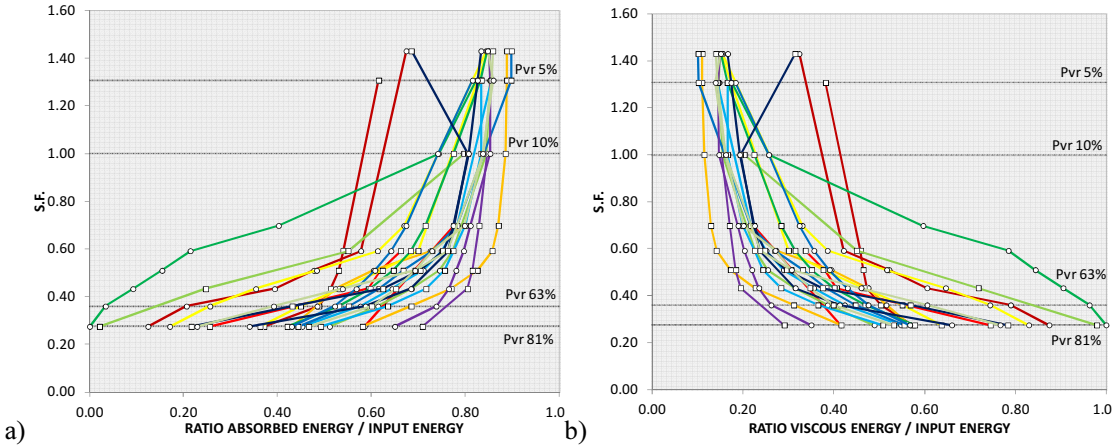


Figure 12. Ratios between: a) the adsorbed and input energies; b) viscous and input energies

## 3 SEISMIC RETROFIT

The IDAs on the current state evidenced several structural problems, such as:

- the building is characterized by a low stiffness in the X direction, both at ground and first floor. The seismic energy dissipation in this direction is mainly obtained through the formation of plastic hinges in the beams and columns;
- in the Y direction, the initial stiffness is sufficient to avoid excessive displacements, but the high slenderness of the bracings implies a insufficiently ductile dissipating mechanism;
- the eccentricity between the bracings and the column in the X direction causes excessive shear forces in the column;
- the structure is characterized by important residual displacements in both directions at the end of the earthquakes (mean values greater than 100 mm for the higher scale factor considered).

On the base of the aforementioned results, a seismic retrofit intervention, using the Steel Self-Centering Device described in [13] is proposed. In the following, after a short description of the device, the pre-sizing of the retrofit is described and its effectiveness is assessed through IDAs. Finally, the influence of the re-centering capability of the SSCD inserted within the structure is investigated trough a parametric analysis.

### 3.1 The steel self-centering device (SSCD)

The SSCD, a complete description of which is available in [13], is made up of three groups of elements, each with specific functions: the Skeleton, the Dissipative Elements and the Pretension Elements. The Skeleton serves to transmit and distribute any external forces between the Dissipative Elements and the Pretension Elements. Figure 13 shows the main Skeleton elements (External Carter, Internal Sliding Frame and Endplates), the Dissipative Elements and the Pretension Elements. The Internal Sliding Frame is positioned within the External Carter.

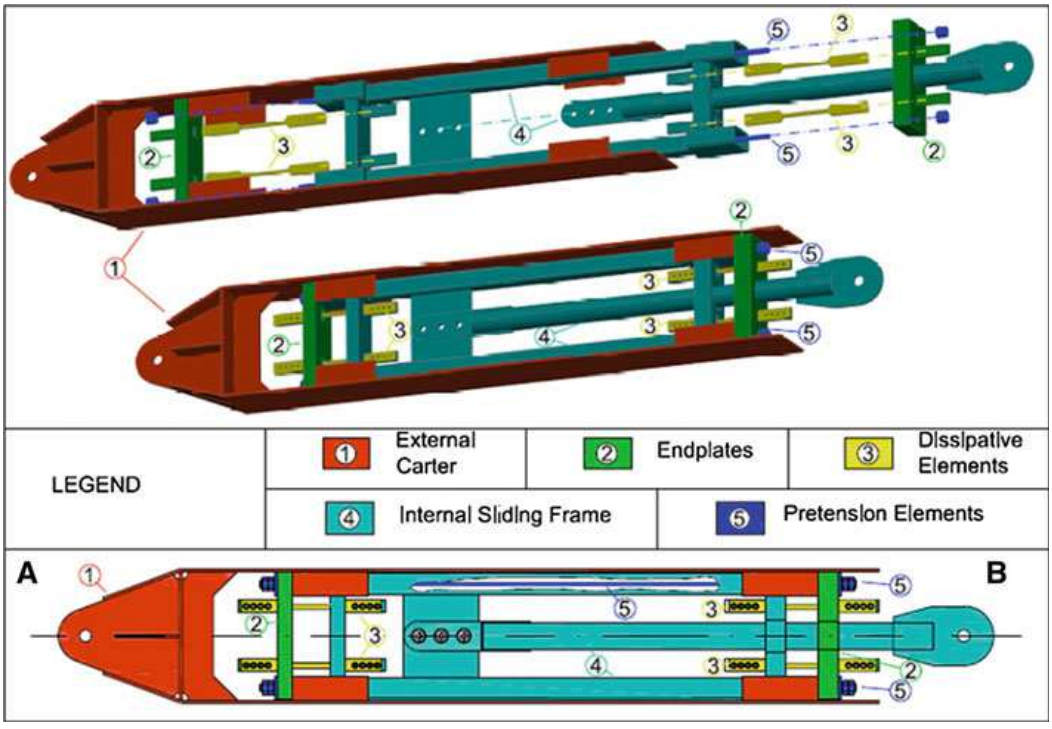


Figure 13. Main elements of the SSCD [13]

The Carter has guide elements that allow the Internal Sliding Frame to move only in the axial direction and, at the same time, serve as stops for the Endplates in the longitudinal direction. The endplates are located in correspondence to the ends of the Internal Sliding Frame. The Dissipative Elements, located within the skeleton, are made up of dog bone shaped steel elements linked to the Internal Carter and the Endplates. They are equipped with a lateral buckling restraining system. The Pretension Elements, made with Prestressing Cables, are located within the Skeleton and linked at both their extremities to the Endplates.

The elements are positioned and connected to each other in order to ensure the same global behavior of the SSCD device under both tension and compression external forces.

Thus, the cyclic behavior of the SSCD is characterized by a flag-shaped hysteretic curve with a residual displacement of zero.

The experimental results carried out in [13] showed the very good capacity of the system in minimizing the residual deformations when the external force drops to zero, see Figure 14.

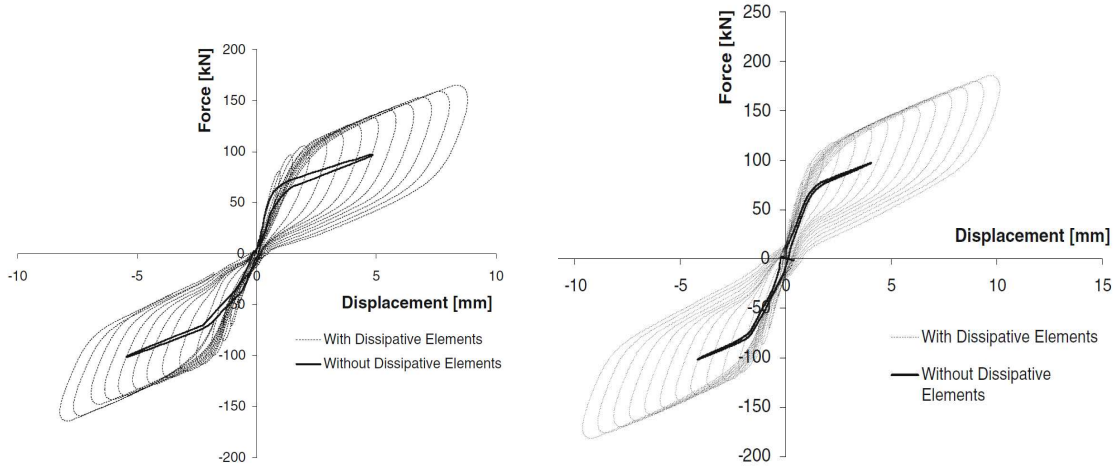


Figure 14. Force-displacement curve of the SSCD with dissipative elements, a) test 1 and b) test 2 [13]

Depending mainly on the value of the ratio between the initial pretension force and the yield strength of the Dissipative Elements, the hysteretic curve of the SSCD may present different shapes, each characterized by different values of the dissipated energy, residual displacement and residual re-centering force, as shown in Figure 15.

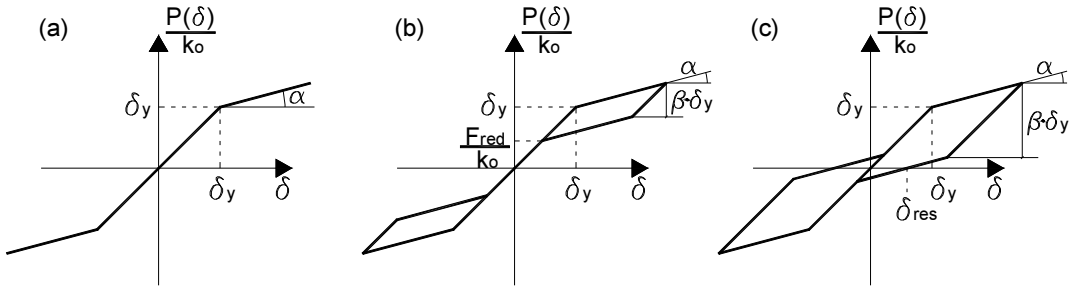


Figure 15. Idealized flag-shaped hysteretic curve normalized by the initial stiffness ko: a) $\beta = 0$, b) $0 < \beta < 1$ and c) $\beta > 1$

The shape of the hysteretic curve can be represented determined by two parameters, $\alpha$ and $\beta$, where $\alpha$ is the ratio between the hardening and the initial stiffness, while $\beta$ reflects the energy dissipation and the system's re-centering capacity [9], which, as mentioned, can be assumed equal to the ratio between the yield strength of the Dissipative Elements and the initial pretension force. A hysteretic curve with $\beta = 0$ can be obtained by using the SSCD without

any Dissipative Element, in which case the device exhibits nonlinear elastic behavior with great re-centering capacity, but no energy dissipation. On the other hand, values of $\beta > 1$ lead to residual displacements (when the external force drops to zero) but also to an higher energy dissipation.

### 3.2 Pre-dimensioning of the SSCD bracings

The SSCD position is assumed limiting, as much as possible, the interferences with the functionality of the building. The SSCD are so introduced, substituting, in the Y direction and at the first floor of the X direction, the existing bracings. To protect also the ground floor elements in the X direction, supplemental SSCD bracings are introduced as schematically shown in Figure 16.

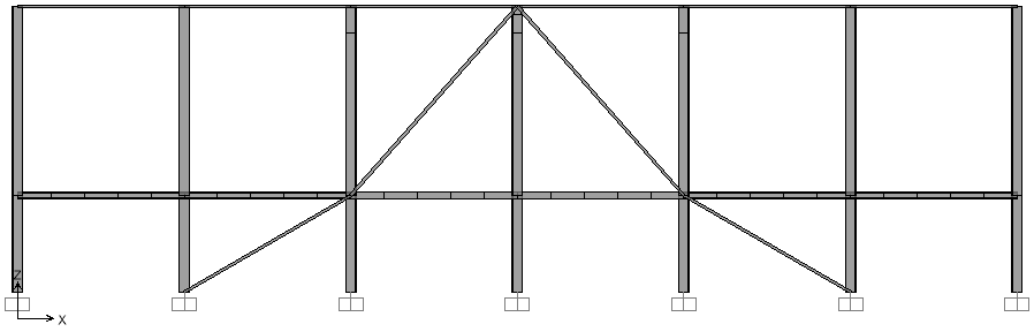


Figure 16. SSCD bracings disposition in the X direction

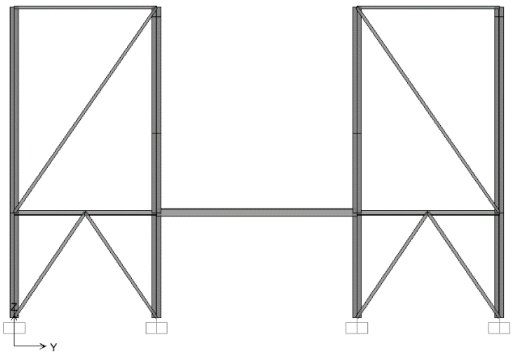


Figure 17. Figure 16. SSCD bracings disposition in the Y direction

The retrofit pre-design is carried out evaluating the characteristics of the SSCD bracings to limit the gravity structure (beams and columns) damage as much as possible. For this reason, the yielding force of the SSCDs are evaluated taking into account the elements resistance to which they are connected. The initial stiffness is estimated imposing a maximum displacement of the gravity structure equal to the one corresponding to the 0.2% of the residual displacement, see Figure 18. The mechanical characteristics of the resulting SSCD are resumed in Table 3.

| Level - direction | Number of SSCD | $k_o$ [kN/mm] | $F_y$ [kN] | α | β |
|---|---|---|---|---|---|
| Ground floor - X | 8 | 72 | 529 | 0.26 | 0.85 |
| First floor - X | 8 | 88 | 848 | 0.26 | 0.85 |
| Ground floor - Y | 28 | 112 | 332 | 0.16 | 0.85 |
| First floor - Y | 14 | 77 | 556 | 0.20 | 0.85 |

Table 3. Mechanical characteristics of the SSCDs


Figure 18. Evaluation of the gravity structure displacement corresponding to the 0.2% of residual displacement in the X direction

## 3.3 IDA results for the retrofitted case

With reference to the levels definition of Figure 7, in the following are reported the main results, in terms of IDA curves.

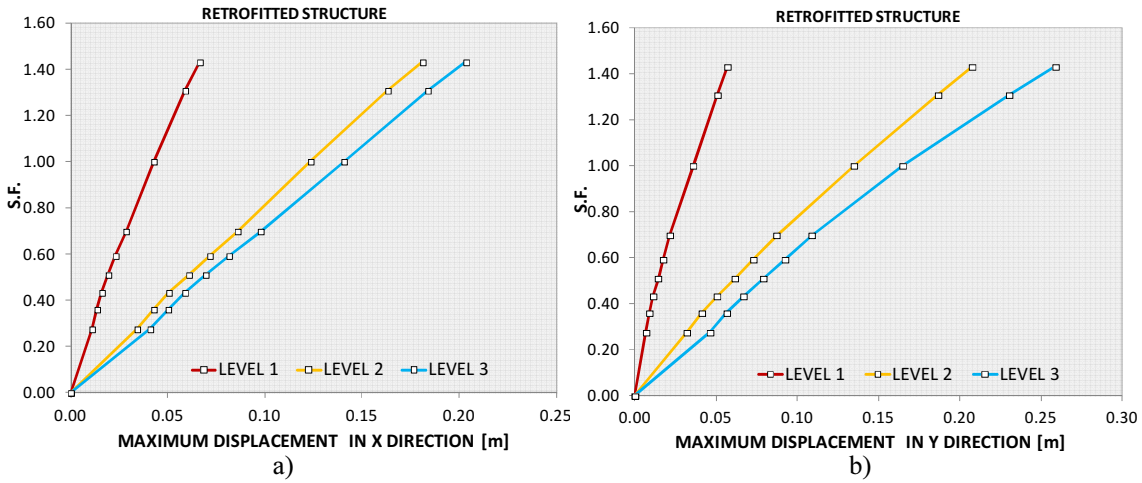


Figure 19. Maximum displacements (mean values) at different level in the a) X and b) Y directions

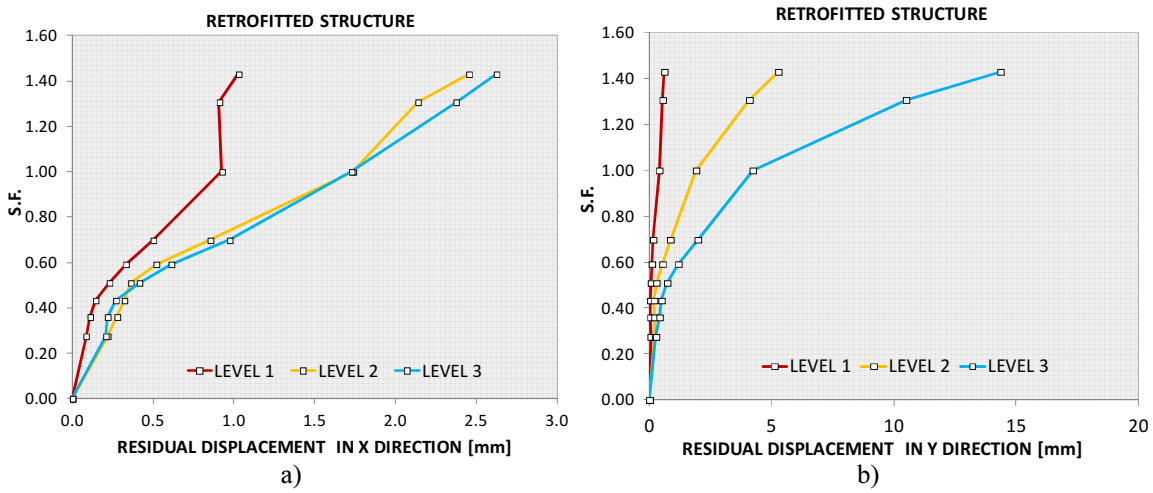


Figure 20. Residual displacements (mean values) at different level in the a) X and b) Y directions

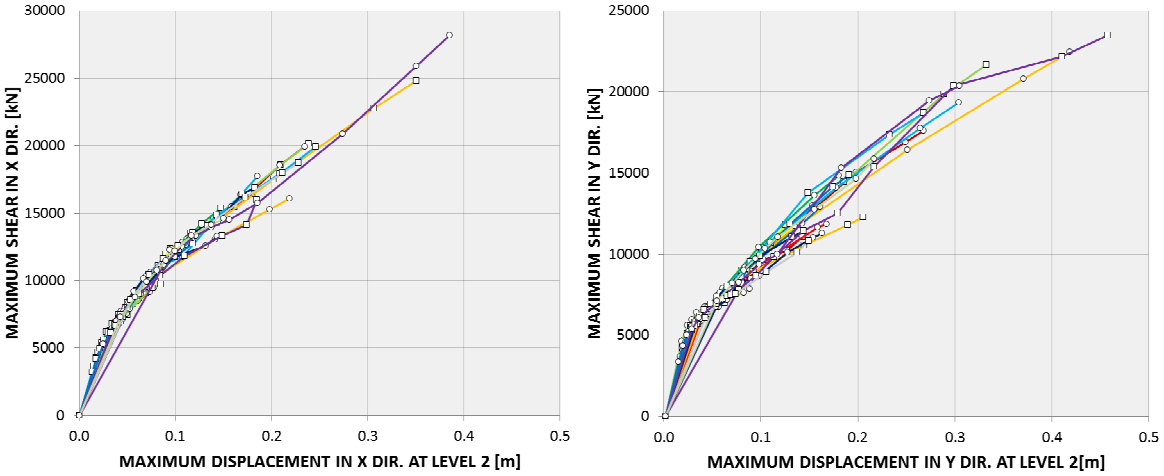


a) b)

Figure 21. Maximum base shear vs maximum displacement at level 2 graph in the a) X direction and b) Y direction

From the analysis of Figure 19 it can be seen that, in both directions, the displacement demand is now equally distributed between the first and second floor. Figure 20 testifies the optimum re-centering capability of the retrofitting solutions: the residual displacements are lower than 3 mm in the X direction and 15 mm in the Y one. In Figure 22 the displacement time-histories for the Ground motion IN445A, SF=1.430, in both the main directions highlights, together with the global hysteretic curves, the differences in terms of maximum and residual displacements in the case of un-retrofitted and retrofitted structure.

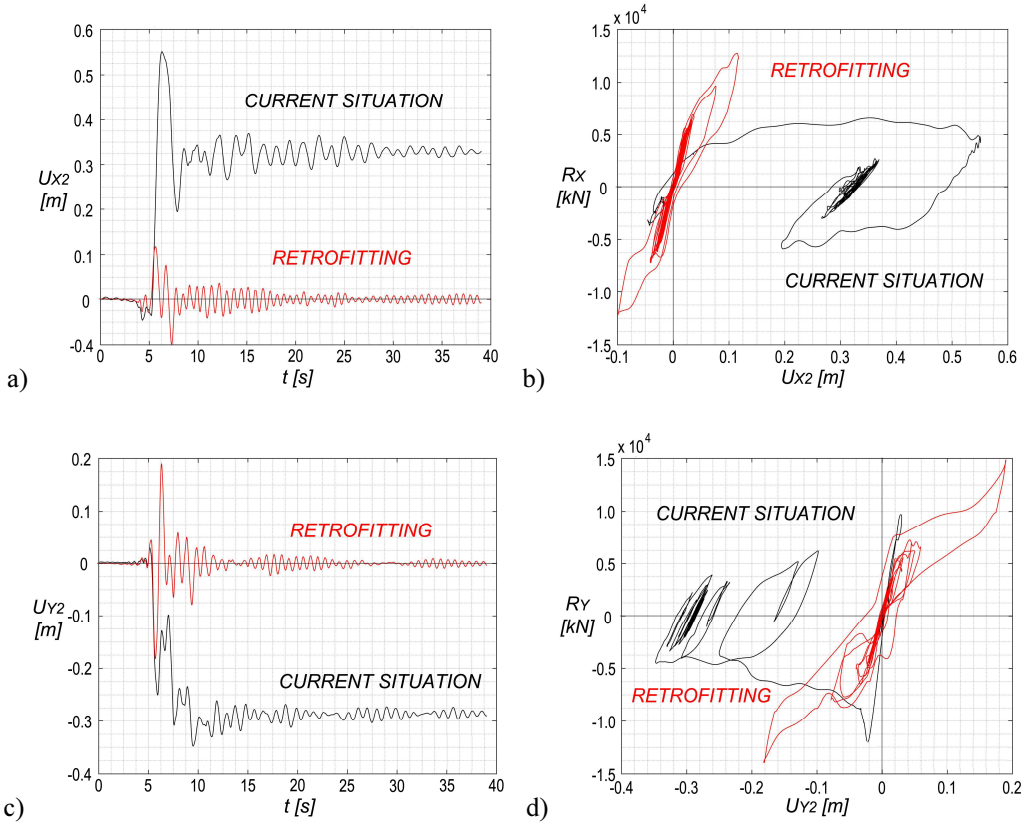


a) b) c) d)

Figure 22. Ground motion IN445A, SF=1.430: level 2 mean displacement time history in a) X and c) Y directions; level 2 mean displacement vs total base shear in b) X and d) direction.

Figure 23 shows, for clarification purpose, the energy time-histories for the IN113A GM for the minimum and maximum scale factor adopted, respectively equal to 0.275 and 1.430. For low value of the seismic action, the gravity structure remains in the elastic field and the energy adsorbed by it is practically equal to zero and all the input energy is dissipated by viscous phenomena, contrarily to the case of the un-retrofitted structure, see Figure 11. When the seismic action and, consequently, the input energy increase, the ratio of energy dissipated by viscous phenomena decreases and the input energy is mainly dissipated by the SSCDs. A low ratio (about 1/5 with respect to the un-retrofitted case) is absorbed by the gravity frame, evidencing so a good level of structural protection.

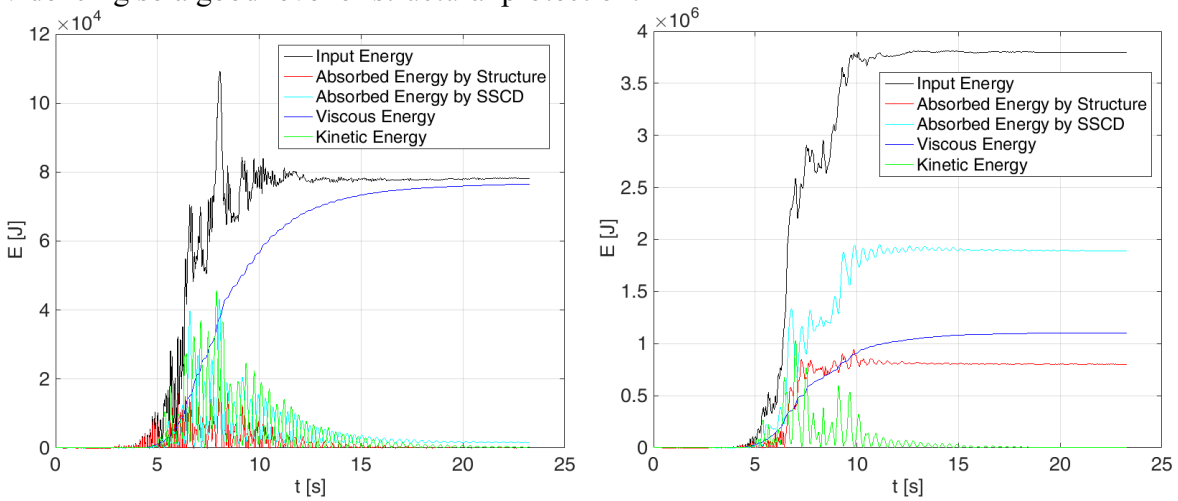


Figure 23. Energy time-histories for the IN113A GM recording: a) SF = 0.275 ; b) SF= 1.430.

The effectiveness of the retrofit can be appreciated analyzing Figure 24 where the energies adsorbed by the gravity structure, representative of the structural damage, and the one dissipated by the SSCDs, both normalized by the input energy, are represented. The structural protection is optimized for values equal to about 0.6, while, for higher values, also the gravity structure dissipates energy, accumulating so damages.

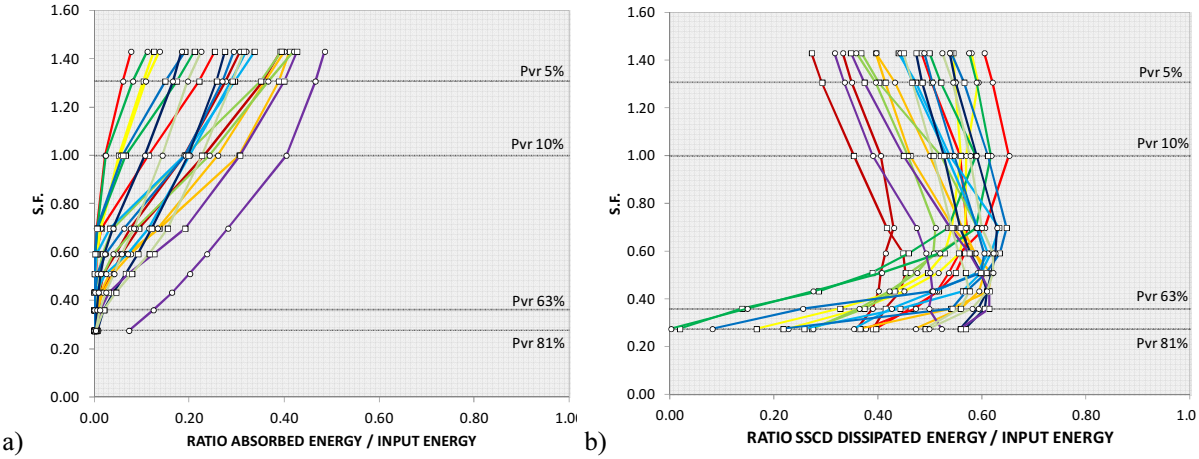


Figure 24. Ratios between: a) the energy adsorbed by the gravity structure and the input one; b) energy dissipated by the SSCDs and input one

## 4 CONCLUSIONS

In the present paper the seismic retrofit of an industrial structure through an innovative self-centering hysteretic dampers is proposed. The need of performing several Incremental Dynamic Analyses required a preliminary simplification phase of the nonlinear model. It resulted that, even for the linear model, the uncertainties related to the missing of a precise knowledge of the infill material mechanical characteristics, does not influence sensibly the dynamic behavior of the whole model. Moreover, for the specific case study analyzed, where the main structural problems are located in the supporting structure, the modelling of the supported silos as elements with equivalent stiffness and mass, provides results, in terms of dynamic responses, very close to one supplied by a refined model.

The execution of IDAs on the nonlinear model of the building in the current state, highlighted several structural problems, even for low value of the seismic action, especially in terms of excessive maximum displacements demand and of residual displacements.

To solve these problems, a retrofit solution using an innovative Steel Self-Centering Device (SSCD) is proposed. The execution of IDAs also in the retrofitted state, highlighted that:

- the dampers minimize, in a very effective way, both the maximum and residual displacements of the structure;
- the gravity structure is completely protected for low-to-mid value of the seismic action, as highlighted by the analysis of the seismic energy components;
- the proposed retrofit solution is optimized for a scale factor, associated to the design spectrum adopted, equal to 0.60. For higher values of scale factors, the building is however able to sustain the seismic action, but some damage is accumulated also in the gravity structure.

Supplemental studies are currently ongoing to evaluate the sensitivity of the building response to the SSCD mechanical characteristics and to compare the efficacy of the innovative damper adopted with respect to the one of a "classical" solution, such as a buckling restrained brace (BRB), not characterized by the presence of a re-centering force, but with an increased energy dissipation capacity [16] [17].

## 5 ACKNOWLEDGMENTS

The research leading to these results has received funding from the European Union's Research Fund for Coal and Steel (RFCS) research programme under grant agreement n° [RFSR-CT-2013-00019] and from the Italian Department of Civil Protection within the Italian Research Project RELUIS-DPC 2014-2018.

## REFERENCES

[1] F. Braga, R. Gigliotti, G. Monti, F. Morelli, C. Nuti, I. Vanzi, W. Salvatore, Post-seismic assessment of existing constructions: evaluation of the shakemaps for identifying exclusion zones in Emilia. *Earthquakes and Structures*, **8**, 37-56, 2014.

[2] F. Braga, R. Gigliotti, G. Monti, F. Morelli, C. Nuti, I. Vanzi, W. Salvatore, Speedup of post earthquake community recovery. The case of precast industrial buildings after the Emilia 2012 earthquake. *Bulletin of Earthquake Engineering*,**12**, 2405-2418, 2014.

[3] F. Braga, F. Morelli, W. Salvatore, A macroseismic approach for the evaluation of seismic risk, J. Kruis, Y. Tsompanakis, B.H.V. Topping eds, *Fifteenth International*

*Conference on Civil, Structural and Environmental Engineering Computing*, Prague, Czech Republic, September 1-4, 2015.

[4] Ministero delle Infrastrutture, Norme Tecniche per le Costruzioni, D.Min. Inf. 14 gennaio 2008, Gazzetta Ufficiale n. 29 of february 4th 2008 - Suppl. Ordinario n. 30, 2008.

[5] European Committee for Standardization. Anti-seismic devices. EN 15129, November 2009.

[6] M. J. N. Priestley, S. Sritharan, J. R. Conley, S. Pampanin, Preliminary results and conclusions from the PRESSS five-storey precast concrete test building. *PCI Journal* **44**(6):42–47, 1999.

[7] C. Christopoulos, A. Filiatrault, B. Folz, C. M. Uang, Post-tensioned energy dissipating connections for moment-resisting steel frames. *ASCE Journal of Structural Engineering* **128**(9):1111–1120, 2002a.

[8] C. Christopoulos, A. Filiatrault, B. Folz, Seismic response of self-centering hysteretic SDOF systems. Earthquake Engineering and Structural Dynamic **31**(5):1131–1150, 2002b.

[9] C. Christopoulos, A. Filiatrault, *Principles of supplemental damping and seismic isolation*. IUSS Press, Pavia, 2006.

[10] C. Christopoulos, R. Tremblay, H. J. Kim, M. Lacerte, Self-centering energy dissipative bracing system for the seismic resistance of structures: development and validation. *Journal of Structural Engineering* **134**(1): 96–107, 2008a.

[11] C. Christopoulos, H. Choi, J. Eronchko, Comparison of the seismic response of steel buildings incorporating self-centering energy dissipative braces, buckling restrained braces and moment resisting frames. In: *Proceedings of the 14th world conference on earthquake engineering*, Beijing, China, 12–17, 2008b.

[12] X. Ma, H. Krawinkler, G. G. Deierlein, Seismic design, simulation and shake table testing of self-centering braced frame with controlled rocking and energy dissipating fuses. J.A. Blume Earthquake Engineering Center, TR 174, Stanford University, (2011).

[13] A. Braconi, F. Morelli, W. Salvatore, Development, design and experimental validation of a steel self-centering device (SSCD) for seismic protection of buildings, *Bulletin of Earthquake Engineering*, **10**, 1915-1941, 2012.

[14] European Committee for Standardization. Eurocode 3: Design of steel structures - Part 1-1: General rules and rules for buildings. En1993-1-1, August 2005.

[15] European Committee for Standardization, Eurocode 8: Design of structures for earthquake resistance - Part 1: General rules, seismic actions and rules for buildings. EN 1998-1, December 2004.

[16] A. Zona, A. Dall'Asta, Elastoplastic model for steel buckling-restrained braces. *Journal of Constructional Steel Research*, **68**(1)118-125, 2012. DOI: 10.1016/j.jcsr.2011.07.017

[17] A. Zona, L. Ragni, A. Dall'Asta, Sensitivity-based study of the influence of brace overstrength distributions on the seismic response of steel frames with BRBs. *Engineering Structures*, **37**(1) 179-192, 2012. DOI: 10.1016/j.engstruct.2011.12.026